

# DNA-Functionalized Gold Nanoparticles in Macromolecularly Crowded Polymer Solutions

Jeehae Shin, Xu Zhang, and Juewen Liu\*

Department of Chemistry and Waterloo Institute for Nanotechnology, University of Waterloo, 200  
University Avenue West, Waterloo, Ontario, Canada N2L 3G1.

Email: liujw@uwaterloo.ca

## Abstract

DNA-functionalized gold nanoparticles (AuNPs) are one of the most commonly used reagents in nanobiotechnology. They are important not only for practical applications in analytical chemistry and drug delivery but also for fundamental understanding of nanoscience. For biological samples such as blood serum or for intracellular applications, the effects of crowded cellular proteins and nucleic acids need to be considered. The thermodynamic effect of crowding is to induce nanoparticle aggregation. But before such aggregation can take place, there might also be a depletion repulsive barrier. Polyethylene glycol (PEG) is one of the most frequently used polymers to mimic the crowded cellular environment. We show herein that while DNA-functionalized AuNPs are very stable in buffer (e.g. no PEG), and citrate-capped AuNPs are very stable in PEG, DNA-functionalized AuNPs are unstable in PEG and are easily aggregated. Although such aggregation in PEG is mediated by DNA, no sharp melting transition typical for DNA-linked AuNPs is observed. We attribute this broad melting to depletion force instead of DNA base pairing. The effects of PEG molecular weight, concentration and temperature have been studied in detail and we also find an interesting PEG phase separation and AuNP partition into the water-rich phase at high temperature.

*This document is the Accepted Manuscript version of a Published Work that appeared in final form in The Journal of Physical Chemistry B, copyright © American Chemical Society after peer review and technical editing by publisher. To access the final edited and published work see <http://dx.doi.org/10.1021/jp310662m>*

## Introduction

With increasing applications of nanomaterials in bioanalytical chemistry and nanomedicine,<sup>1-8</sup> it is crucial to gain a detailed understanding of their properties in biological fluids. For example, biosensors and drug delivery vehicles optimized in buffer may behave very differently inside a cell. One of the most important cellular features is the presence of concentrated proteins and nucleic acids, which occupy about 20-40% of a live cell's volume.<sup>9</sup> They create a crowded environment imparting depletion force on colloidal particles.<sup>10-13</sup> Unlike other intermolecular forces, such as electrostatic, van de Waals and hydrophobic interactions, depletion force exists only in crowded polymer solutions.<sup>14</sup> A non-adsorbing polymer loses its configuration entropy when it approaches a particle surface. To avoid this, the polymer chain tends to stay away from the surface and thus creating a depletion zone around the particle (Figure 1A, the zones defined by the black dashed lines). The width of the depletion zone is equal to the radius of the polymer. If the depletion zones of two particles overlap, it creates a thermodynamically favourable situation to generate more free volume for the polymer. In this case, the depletion zone has no polymer and the osmotic pressure caused by the surrounding polymers pushes the two particles together, which is known as depletion attraction force or depletion flocculation.

Before depletion attraction can take place, when two nanoparticles approach each other in a polymer solution, they may experience a repulsive depletion force, which increases the colloidal stability and is called depletion stabilization. The origin of depletion repulsion is related to the difficulty of transporting the polymers between the particles against a deep osmotic pressure gradient. At high polymer concentration, it is even more difficult to push the polymer chains out of the gap region between two particles (e.g. the red polymer chain in Figure 1B). Depletion attraction is thermodynamically favored; in other words, depletion repulsion is only a kinetic phenomenon.<sup>15</sup> An energy diagram of depletion attraction and repulsion is shown in Figure 1C.

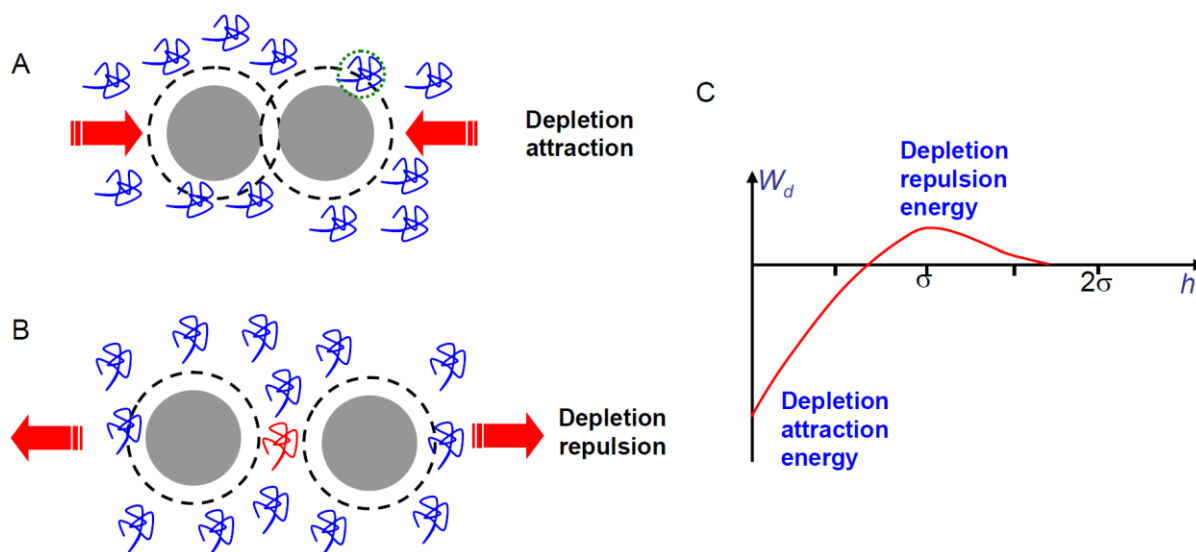


**Figure 1.** Schematics of depletion attraction (A) and depletion repulsion (B). The depletion zone on the particles are indicated by the black dashed lines and its width is equal to the radius of the polymer. The size of the polymer is indicated by the green dashed line. In (B), to push the red polymer out of the gap region is difficult when the polymer concentration is very high, creating the depletion repulsion force. (C) Depletion potential between two particles mediated by polymers modeled as hard spheres. Drawing is not to scale. The  $x$ -axis is the distance between two particles and the unit is the diameter of the polymer depleting agent.

Colloidal stability in crowded polymers is typically monitored by measuring their rheological properties, microscopic arrangements, or using dynamic light scattering.<sup>16-19</sup> Most of these techniques require a high particle concentration, large particle size, expensive instruments or a long measurement time. Silica and latex beads are among the most studied particles. However, these experimental conditions may not directly relate to real biosensing or drug delivery applications. In this regard, studying DNA-functionalized AuNPs is attractive for both practical applications and for fundamental colloidal science. On the applications side, the DNA layer serves as a targeting ligand or sensing moiety (e.g. aptamers), while the AuNP core is highly biocompatible and allows a high DNA loading capacity. On the fundamental side, AuNPs possess extremely high extinction coefficients, allowing

convenient optical observation at low nM and even pM concentration. The aggregation of AuNPs is accompanied with a red-to-blue color transition and thus no instrument is required. The DNA layer provides both charge and steric stabilization. Finally, programmable and reversible interactions are also possible because of DNA.<sup>20</sup>

We recently reported that high molecular weight (MW) PEG could afford remarkable colloidal stability to citrate-capped AuNPs (i.e. no DNA) against salt due to depletion repulsion.<sup>21</sup> The stability of DNA-capped AuNPs in PEG might be different because of the DNA layer. A number of intermolecular forces come into play including electrostatic repulsion by DNA, attractive interactions between DNA bases, van de Waals force and depletion force. In addition, specific AuNP interaction can be achieved by adding linker DNA. In this work, we explore the stability of DNA-capped AuNPs in a diverse range of PEG solutions, thus tuning the strength of the depletion force. Our result revealed many interesting physical chemistry behaviors such as diminished colloidal stability, phase separation of PEG and partition of AuNPs. Most strikingly, we found that PEG can lead to the loss of the sharp melting transition that is typically seen for DNA-linked AuNPs.

## 1. Materials and Methods

**Chemicals.** All the PEG samples (MW = 200, 400, 2k, 4k, 8k, and 20k) were purchased from VWR. AuNPs (13 nm diameter) were synthesized based on the standard citrate reduction procedures,<sup>22</sup> and its concentration was estimated to be ~10 nM. The DNA samples were purchased from Integrated DNA Technologies Inc (Coralville, IA). The linkage between DNA and AuNPs are shown in Figure S1. Most experiments involved only the sample in Figure S1A, where a 5'-thiolated 12-mer DNA was attached to AuNPs. For the melting experiment in Figure 5E of the paper, the construct in Figure S1B was used. The DNA sequences for Figure 3C are shown in Figure S1C. NaCl, trisodium citrate and 4-(2-hydroxyethyl) piperazine-1-ethanesulfonate (HEPES) were purchased from Mandel Scientific (Guelph,

Canada). Tris(2-carboxyethyl)phosphine (TCEP), was purchased from Sigma-Aldrich. Milli-Q water was used for all experiments.

**Prepare DNA-functionalized AuNPs.** To achieve stable DNA-capped AuNPs, thiolated DNA was first activated by 100-fold excess of TCEP at pH 5 (50 mM acetate buffer) for 1 hr to cleave the disulfide bond. The mixture was purified using a C<sub>18</sub> desalting column to completely remove TCEP and the cleaved small thiol compound. The resulting DNA was lyophilized and then re-dissolved in 5 mM HEPES (pH 7.6). This activated DNA and AuNPs were mixed at a ratio of 400:1 for 1 hr before 50 mM NaCl was added. After another 2 hrs, another 150 mM NaCl was added and the mixture was allowed to age overnight. Different from the previous protocol,<sup>23</sup> no HEPES was added to adjust pH to neutral since we found that lower pH is more favourable for DNA attachment.<sup>24</sup> The actual pH was tested to be between 5-6. To prepare DNA-linked AuNP aggregates as shown in Figure S1B, 10 nM of each DNA-capped AuNPs were mixed with 200 nM linker DNA in 300 mM NaCl, 20 mM HEPES, pH 7.6. The color of the solution changed to purple in a few minutes and the reaction was allowed to continue overnight. The next day, the sample was briefly centrifuged to remove the supernatant and the pellet was re-dispersed in 100 mM NaCl, 20 mM HEPES, pH 7.6.

**AuNP stability.** Most of the reactions were carried out in a final volume of 100  $\mu$ L. All the PEG stock solutions were 20% (w/w). For citrate-capped AuNPs,  $\sim$ 50  $\mu$ L of the 10 nM AuNPs and 50  $\mu$ L of PEG were mixed. NaCl was added at the last. The color of the AuNPs was recorded using a digital camera and sometimes also using a UV-vis spectrophotometer (Agilent 8453A).

**Temperature-dependent studies.** For visual observation, the microcentrifuge tubes were heated in a dry bath and the temperature was determined using a thermometer. The incubation time was usually around 2 min at each designated temperature. For quantitative study, the spectrophotometer was used and the temperature was controlled by an external water bath. The temperature was increased by 1-2  $^{\circ}$ C and the holding time at each temperature was 2 min.

**PEG adsorption.** To measure PEG adsorption, 100  $\mu\text{L}$  of 10 nM citrate-capped or DNA-capped AuNPs were respectively mixed with 200 nM FAM-labeled PEG 10k. After 10 min incubation at room temperature, the samples were washing three times with repeated centrifugation at 15,000 rpm for 12 min, removal of the supernatant and adding 10 mM HEPES (pH 7.6). Finally, the AuNPs were dispersed in 70  $\mu\text{L}$  of 15 mM KCN and the AuNPs were dissolved in a few minutes. The fluorescence was measured by mixing 5  $\mu\text{L}$  of the dissolved AuNP samples with 95  $\mu\text{L}$  of 50 mM HEPES (pH 7.6) using a microplate reader (Infinite F200 Pro, Tecan).

## Results and Discussion

**Effect of PEG and salt on AuNP stability.** Our 13 nm AuNPs were synthesized by the well-established citrate reduction reaction.<sup>22</sup> The as-synthesized AuNPs can be stably dispersed for many years because of the charge stabilization from the weakly adsorbed citrate ions. However, addition of more than 30 mM NaCl resulted in instantaneous aggregation due to charge screening (see Supporting Information), where AuNPs can approach each other to experience van de Waals attractive force.<sup>25</sup> This aggregation process is accompanied with a color change from red to blue. One way to stabilize such citrate-capped AuNPs is to add a high MW PEG (Figure 2A).<sup>21</sup> For example, little color change was observed with up to 0.7 M NaCl in the presence of 10% (w/w) PEG 20k (Figure 2B). The UV-vis spectra of the samples showed a sharp surface plasmon peak at 520 nm, confirming the lack of AuNP aggregation. Depletion repulsion played a crucial role in this case.<sup>21</sup> An alternative and commonly used way to stabilize and functionalize AuNPs is to displace the surface citrate with a polymer such as a thiolated DNA (Figure 2C). For example, when functionalized with DNA1 (see Figure S1 for sequence), adding up to 2.9 M NaCl did not cause color change and this was also confirmed by UV-vis spectroscopy (Figure 2D). The samples with high NaCl concentrations show slightly lower extinction values due to the adsorption of some AuNPs by the wall of the microcentrifuge tube, while the AuNPs

in solution remained fully dispersed. Therefore, either using PEG as a solvent component or attaching DNA provides good protection to AuNPs. It needs to be re-emphasized that stabilization by PEG is related to the depletion effect while stabilization by DNA is because of charge and steric effect. Next we tested the stability of DNA-capped AuNPs in 10% PEG 20k (Figure 2E). Surprisingly, instead of being even more stable, the stability of the conjugate was significantly decreased. For example, 300 mM NaCl induced a blue color (Figure 2F). Therefore, additional attractive forces must be imparted by PEG to push these DNA-capped AuNPs together.

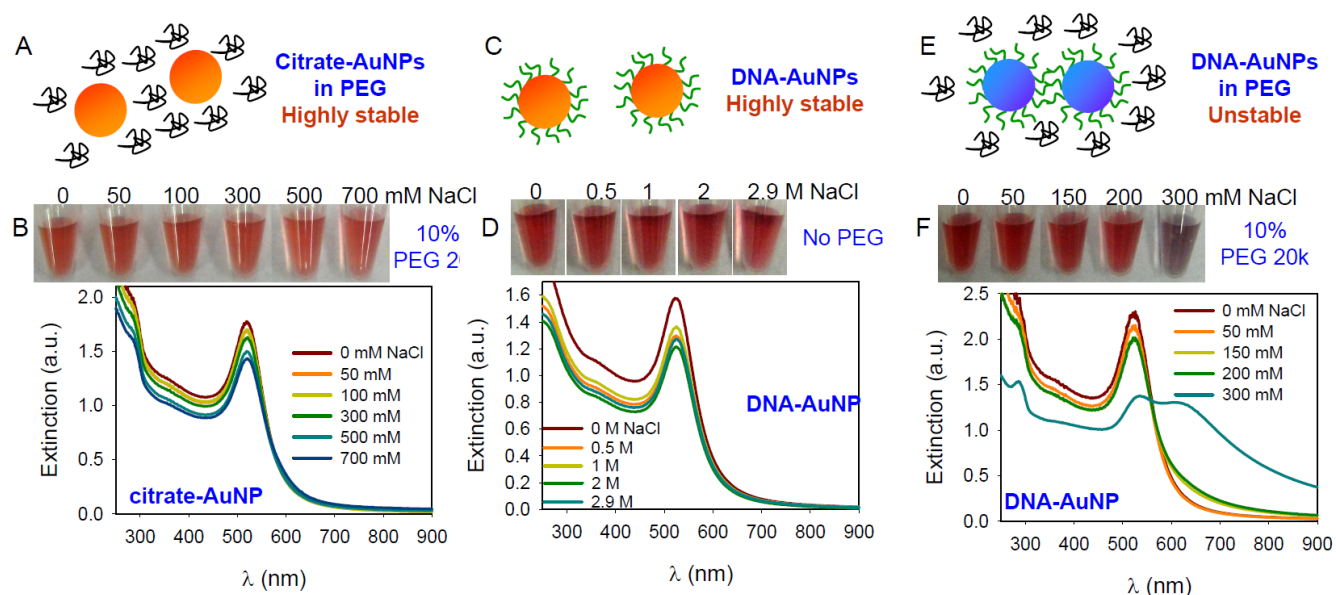


**Figure 2.** (A, C, E) Schematics of the aggregation state of AuNPs in the highest salt concentration tested in (B, D, F), respectively. (B) Photographs and UV-vis spectra of citrate-capped AuNPs dispersed in 10% PEG 20k with increasing concentrations of NaCl. (D) DNA-functionalized AuNPs in the absence of PEG. (F) DNA-functionalized AuNPs in 10% PEG 20k.

To better understand the colloidal stability of DNA-functionalized AuNPs, we varied the concentration and MW of PEG. As shown in Figure 3A, using 1 M NaCl, a slight shift in the UV-vis spectrum was observed with just 5% PEG 20k, although the color remained quite red. A blue color

indicating extensive aggregation was observed with 7% or 10% PEG 20k. The depletion attractive energy ( $W_d$ ) can be written as

$$\frac{W_d}{kT} = -3 \frac{R}{\sigma} \left( \phi + \frac{\phi^2}{5} \right) \quad (1)$$

where  $R$  and  $\sigma$  are the radius of AuNP and diameter of PEG, respectively, and  $\phi$  is the volume fraction of PEG.<sup>12,14</sup> This energy corresponds to the energy shown in Figure 1C when the two AuNPs touch each other and PEG is completely depleted. The negative sign indicates the force is attractive. A bigger negative value means stronger attractive force between particles, thus the particles are more prone to aggregation. For this equation, PEG is modeled as hard spheres. Since  $\phi$  is proportional to the concentration of PEG, the attractive force is stronger with higher PEG concentration, which explains the trend in Figure 3A.

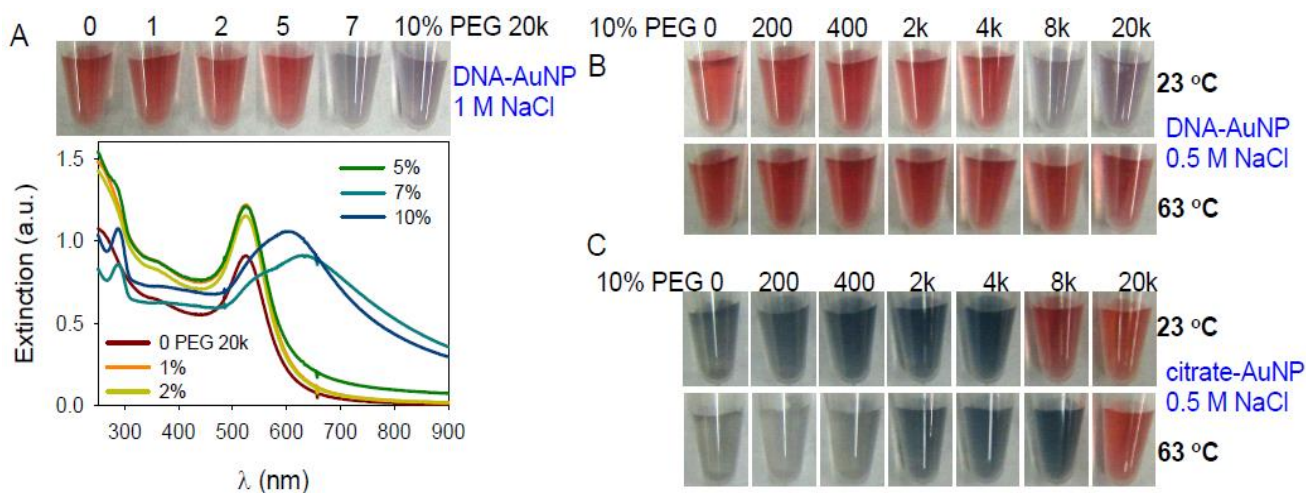


**Figure 3.** (A) Photograph and UV-vis spectra of DNA-functionalized AuNPs in 1 M NaCl with increasing concentrations of PEG 20k. DNA-functionalized AuNPs (B) and citrate-capped AuNPs (C) in 10% of PEG with various MW at room temperature and at 63 °C.

Next we fixed the PEG concentration to be 10% (w/w), while the PEG MW was varied. The color of AuNPs turned blue only when the MW was 8000 or larger (Figure 3B). We calculated using



Eq (1) the depletion energy to be  $-3.5kT$  for 10% PEG 8k, while all the lower MW PEGs have lower energy (see Supporting Information), with the next highest being PEG 2000 ( $2.2 kT$ ). Eq (1) cannot be directly applied to 10% PEG 20k since it reaches the semi-dilute region at  $\sim 5.6\%$ ,<sup>26</sup> where the PEG chains start to overlap and the hard sphere model breaks down.

**Reversibility test.** In our recent work to study the melting of DNA duplex in DNA-linked AuNPs, we found that even PEG 200 can exert a stabilization effect.<sup>27</sup> In that case, DNA hybridization force was playing a dominating role. In the current work, the starting state of AuNPs was dispersed. Without a linker DNA, the depletion force alone needs to push the AuNPs together, explaining the strict requirement in the MW and concentration of PEG. To test reversibility, these samples were heated to  $63\text{ }^\circ\text{C}$ . Color changing from blue to red was observed for the PEG 8k and 20k samples, suggesting the DNA-capped AuNPs were reversibly aggregated (Figure 3B). To further confirm reversibility, we centrifuged the aggregated sample and removed the supernatant. Red color indicative of dispersed AuNPs was observed when water was added (see Supporting Information). This experiment eliminates possible artifacts associated with heating.

It is interesting to note that without DNA, citrate-capped AuNPs can survive 500 mM NaCl only if the PEG MW is greater than 8k (Figure 3C), which is opposite to the trend in Figure 3B for DNA-capped AuNPs. Citrate-capped AuNPs are only stabilized by the weak charge repulsion. With 500 mM NaCl, this charge repulsion is effectively screened. Only high MW PEGs can produce a sufficiently high depletion repulsion barrier to retain AuNP stability. If the particles have enough thermal energy to cross the depletion barrier (e.g. at  $63\text{ }^\circ\text{C}$ ), aggregation can still take place. For example, the AuNPs dispersed in PEG 8k changed color from purple to blue after heating (Figure 3C). This heating however did not provide enough energy to aggregate AuNPs in PEG 20k. It needs to be emphasized that the aggregation of citrate-capped AuNPs is irreversible. Once aggregated, a number of

other attractive forces including van der Waals force and even metallic bond formation become dominating. As a result, heating cannot provide sufficient energy to separate them. The surface DNA layer also appeared to reduce the depletion repulsion barrier height; under the condition that citrate-capped AuNPs remains stable, DNA-capped AuNPs aggregated (e.g. with PEG 8k and 20k in Figure 3B). Since the DNA layer avoids direct metallic gold contact and also reduces their van der Waals attraction, only moderate energy is needed to separate DNA-capped AuNPs (e.g. overcome the depletion attraction). We show here that heating increases the entropic effect of the whole system, which is sufficient to re-disperse the AuNPs at high temperature.

As shown in Figure 1B, depletion repulsion is related to the difficulty to push PEG chains out of the gap region between two approaching nanoparticles. We have previously shown that AuNPs could weakly adsorb PEG.<sup>21,28</sup> This adsorption may increase the difficulty to push the PEG out of the gap. When the surface of the AuNPs is capped with DNA, PEG can hardly interact directly with the AuNP surface and DNA has been reported to repel PEG, which may explain the reduced depletion repulsion barrier in the DNA case. To test this hypothesis, we mixed FAM-labeled PEG 10k with citrate-capped and also with DNA-capped AuNPs. After repeated centrifugation and washing, all non-adsorbed FAM-labeled PEG was removed and the AuNPs were dissolved by KCN. The fluorescence of the final solutions was measured. As shown in Figure 4, very strong fluorescence was observed with citrate-capped AuNPs but none of the DNA-capped AuNPs showed PEG adsorption, confirming the lack of affinity between PEG and DNA. This difference may explain the lower depletion energy barrier in the presence of DNA.

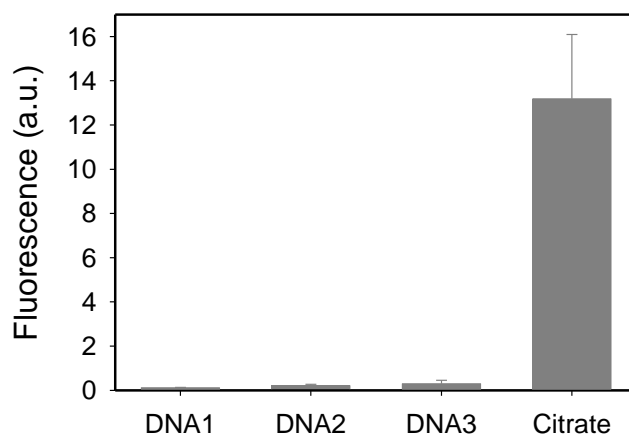


**Figure 4.** Measurement of adsorbed FAM-labeled PEG 10k by DNA-capped or citrate-capped AuNPs. A stronger fluorescence indicates more adsorbed PEG.

**Broad melting transition.** Using a linker DNA, DNA-functionalized AuNPs can be assembled to form aggregates. If the DNA on AuNPs is self-complementary, aggregation takes place even without linker DNA.<sup>29</sup> In both cases, sharp melting transitions are the standard feature of such DNA-linked AuNPs, where co-operative melting of the multiple DNA linkages has been proposed to be responsible for such sharp melting transitions.<sup>30-32</sup> In our current system, DNA-capped AuNPs also aggregated in PEG even without linker DNA and we wonder if the sharp transition is still maintained. For this purpose, heated DNA-capped AuNPs were gradually heated in 10% PEG 8k or 20k samples with 0.5 M NaCl. UV-vis spectra of the sample in PEG 8k are shown in Figure 5A and the spectra continued to evolve in this whole temperature range. We chose to monitor the 260 nm since it has a relatively large change in the melting process. It needs to be pointed out that the hyperchromic effect of DNA melting contributes very little to the 260 nm extinction change and the surface plasmon coupling of AuNPs is the main contributor.<sup>30,33</sup> By plotting the extinction value at 260 nm as a function of temperature (Figure 5B, black dots), we can see that the melting transition was indeed very broad, spanning ~40 °C. PEG 20k also showed a broad melting transition (red dots) but the overall temperature shifted to higher

temperature, indicating that the AuNPs were more stably aggregated in PEG 20k. A scheme of this melting process is shown in Figure 5C. For comparison, we tested typical DNA-linked AuNPs (Figure 5D) in the presence or absence of PEG. To avoid non-specific interactions mediated by PEG, we only used 50 mM NaCl. Compared to the melting in the absence of PEG, both PEG 8k and PEG 20k increased the  $T_m$  by  $\sim 10$  °C and sharp melting transitions were observed for all the samples (Figure 5E). In this case, the increased  $T_m$  is due to the depletion force acting on AuNPs, which is coupled to the melting of DNA. The sharp transition indicates that DNA hybridization is still responsible for the integrity of the AuNP structure.

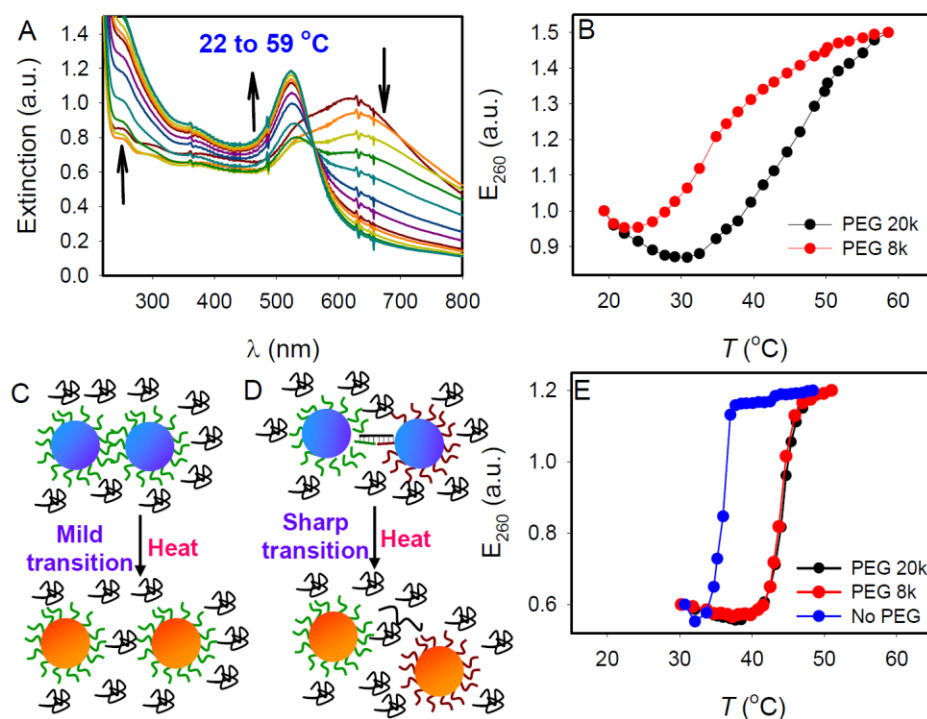


**Figure 5.** (A) UV-vis spectra of DNA-functionalized AuNPs dispersed in 10% PEG 8k and 0.5 M NaCl. The arrow heads point the direction of spectral change at those wavelengths. Melting curves (B) and scheme (C) of DNA-capped AuNPs in 10% PEG with 0.5 M NaCl without linker DNA. Melting curves (E) and scheme of DNA-linked AuNPs in 0 or 10% PEG with 50 mM NaCl.

This comparison also allows us to deduce that the melting in Figure 5B is not caused by denaturing the DNA but by the polymer action. In other words, under our experimental conditions, DNA does not form base pairs with each other and the aggregation is from a pure depletion force acting on AuNPs. This attractive depletion force is balanced by electrostatic repulsion between DNA and thus NaCl is needed to screen the charge repulsion. At high temperature, the overall entropy effect becomes more important and leads to the disassembly of the nanoparticle aggregates. As calculated above, the depletion force is just a few  $kT$ , which is much weaker than DNA base pairing energy. When AuNPs are linked by DNA base pairing interactions, heating leads to the melting of DNA, after which the AuNPs already have sufficient energy to be freely dispersed.

**PEG phase separation and partition of AuNPs.** In the above studies, we only heated the samples to  $\sim 60$  °C. We found an interesting phase separation effect as the temperature was further increased. For example, three samples were prepared all containing 10% PEG 20k but with 0.5, 1, or 1.5 M NaCl. At room temperature, all the samples were aggregated and blue (Figure 6A). Heating the sample to 52 and 62 °C produced a red color for the 0.5 M NaCl sample while the two higher salt samples are purple. At 72 °C, the 1.5 M NaCl sample showed phase separation, where the lower critical solution temperature (LCST) of PEG 20k was reached. PEG is a quite hydrophilic polymer, but at high temperature and high salt, the hydrogen bonding between water and the polymer is disrupted, leading to this phase separation. The DNA-AuNP conjugate is in the upper water rich phase while the PEG polymer has a higher density and is at the bottom. Heating to 92 °C resulted in phase separation also for the lower salt samples. Apparently the LCST of PEG is a function of salt concentration. At high salt, the water/PEG interaction is less favored and PEG more easily interacts with itself. PEG phase separation from water has been previously observed upon addition of concentrated salt.<sup>34-36</sup> Since AuNPs partition in the

water phase with a high efficiency (e.g. the PEG layer is clear), this might be useful for analytical applications, in particular, when a lower LCST polymer is used such as poly(N-isopropylacrylamide).

We further tested the reversibility of this phase separation process. After phase separation, the system can be fully mixed by shaking at a lower temperature and the color gradually changes back to purple/blue (Figure 6B). Heating the samples again generated phase separation. This is also a strong indication that the DNA is stably attached to AuNPs. The phase separation and the partition of AuNPs are independent of the DNA sequence. We have tested another six thiolated DNA and all showed the same behavior at high temperature (Figure 6C).

To confirm that the bottom layer is rich in PEG, we designed the following two experiments. First, 150  $\mu\text{L}$  of 20% PEG 20k and 400  $\mu\text{L}$  of water with a final of 1 M NaCl was mixed. To this mixture a final of 0.4  $\mu\text{M}$  of FAM-labeled PEG 10k was added and the solution was thoroughly mixed. After heating in boiling water, we found that the fluorescence was mainly in the bottom layer and this bottom layer has a smaller volume fraction in the tube (Figure 6D). If we assume that PEG 10k tends to partition into the PEG rich phase, it suggests that the bottom layer is rich in PEG. To further confirm this, we prepared another sample. After phase separation, a small volume of the top and bottom layer was respectively transferred to another tube. To each tube, the same volume of DNA-capped AuNPs dispersed in water was added and mixed. After heating, phase separation was observed only for the sample with the bottom fraction from the previous phase separated sample (Figure 6E), confirming that the bottom layer is rich in PEG.

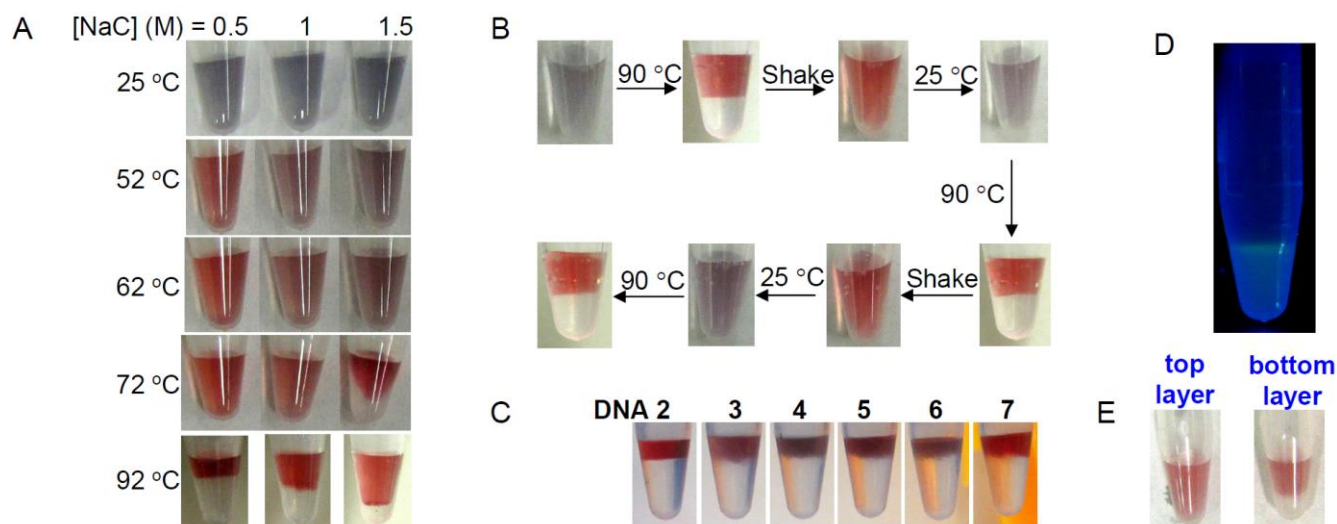


**Figure 6.** (A) Photographs of DNA-capped AuNPs dispersed in 10% PEG 20k with various concentrations of NaCl. At high temperature, the color change to red indicating dis-assembly of AuNPs and phase separation also occurred. (B) Repeated phase separation, re-dispersing and aggregation of DNA-capped AuNPs in 10% PEG 20k with 1 M NaCl. (C) Phase separation with other DNA sequences. (D) Fluorescence image of a sample after heating containing a small fraction of PEG 20k and FAM-labeled PEG 10k. The bottom layer with a smaller volume is fluorescent suggests that the bottom layer is PEG rich. (E) Pictures of DNA-capped AuNPs mixed with the top or the bottom layer of a phase separated PEG sample after heating. The bottom layer fraction showed phase separation suggests that the bottom layer is rich in PEG.

## Conclusions

In summary, this work has revealed many interesting physical chemistry behaviors of DNA-capped AuNPs in a crowded polymer solution. This has practical implications when the use of these materials for drug delivery and *in vivo* sensing is concerned. For the fundamental physical chemistry, we observed the following new phenomena. First, the surface DNA facilitates AuNPs to cross the depletion repulsion barrier. Beyond the repulsive barrier, depletion attraction force takes place, leading

to the loss of colloidal stability even in the absence of linker DNA. With the protection of DNA, such aggregation is reversible and removal of PEG allows re-dispersing of AuNPs. Second, since these AuNPs were aggregated by depletion force instead of DNA base pairing interaction, heating the sample leads to very mild melting transitions, which is in sharp contrast to that for normal DNA-mediated melting. This suggests a different way to assemble such DNA-functionalized AuNPs and its underlying physical chemistry principle is also different. Finally, PEG could undergo phase transition in high salt concentration and at high temperature. DNA-functionalized AuNPs remain to be quite hydrophilic under this condition and partition into the water rich phase.

### **Acknowledgment**

Funding for this work is from the University of Waterloo, the Canadian Foundation for Innovation, and the Natural Sciences and Engineering Research Council (NSERC) of Canada and the Early Researcher Award from the Ontario Ministry of Research and Innovation.

**Supporting Information.** DNA sequences, additional calculations and salt induced AuNP aggregation.

“This material is available free of charge via the Internet at <http://pubs.acs.org>.”

### **References:**

- (1) Rosi, N. L.; Mirkin, C. A. *Chem. Rev.* **2005**, *105*, 1547-1562.
- (2) Giljohann, D. A.; Seferos, D. S.; Daniel, W. L.; Massich, M. D.; Patel, P. C.; Mirkin, C. A. *Angew. Chem. Int. Ed.* **2010**, *49*, 3280-3294.
- (3) Saha, K.; Agasti, S. S.; Kim, C.; Li, X.; Rotello, V. M. *Chem. Rev.* **2012**, 2739–2779.
- (4) Liu, J.; Cao, Z.; Lu, Y. *Chem. Rev.* **2009**, *109*, 1948–1998.
- (5) Wang, H.; Yang, R. H.; Yang, L.; Tan, W. H. *ACS Nano* **2009**, *3*, 2451-2460.
- (6) Zhao, W.; Brook, M. A.; Li, Y. *ChemBioChem* **2008**, *9*, 2363-2371.



- (7) Li, D.; Song, S. P.; Fan, C. H. *Acc. Chem. Res.* **2010**, *43*, 631-641.
- (8) Lee, O. S.; Prytkova, T. R.; Schatz, G. C. *J. Phys. Chem. Lett.* **2010**, *1*, 1781-1788.
- (9) Zimmerman, S. B.; Minton, A. P. *Ann. Rev. Biophys. Biomol.* **1993**, *22*, 27-65.
- (10) Asakura, S.; Oosawa, F. *J. Chem. Phys.* **1954**, *22*, 1255-1256.
- (11) Asakura, S.; Oosawa, F. *Journal of Polymer Science* **1958**, *33*, 183-192.
- (12) Mao, Y.; Cates, M. E.; Lekkerkerker, H. N. W. *Physica A* **1995**, *222*, 10-24.
- (13) Miyoshi, D.; Sugimoto, N. *Biochimie* **2008**, *90*, 1040-1051.
- (14) Lekkerkerker, H. N. W.; Tuinier, R. *Colloids and the Depletion Interaction* New York, 2011.
- (15) Semenov, A. N. *Macromolecules* **2008**, *41*, 2243-2249.
- (16) Ogden, A. L.; Lewis, J. A. *Langmuir* **1996**, *12*, 3413-3424.
- (17) Bakandritsos, A.; Psarras, G. C.; Boukos, N. *Langmuir* **2008**, *24*, 11489-11496.
- (18) Kim, S. Y.; Zukoski, C. F. *Langmuir* **2011**, *27*, 5211-5221.
- (19) Edwards, T. D.; Bevan, M. A. *Macromolecules* **2012**, *45*, 585-594.
- (20) Storhoff, J. J.; Mirkin, C. A. *Chem. Rev.* **1999**, *99*, 1849-1862.
- (21) Zhang, X.; Servos, M. R.; Liu, J. *J. Am. Chem. Soc.* **2012**, *134*, 9910-9913.
- (22) Storhoff, J. J.; Elghanian, R.; Mucic, R. C.; Mirkin, C. A.; Letsinger, R. L. *J. Am. Chem. Soc.* **1998**, *120*, 1959-1964.
- (23) Liu, J.; Lu, Y. *Nat. Protoc.* **2006**, *1*, 246-252.
- (24) Zhang, X.; Servos, M. R.; Liu, J. *J. Am. Chem. Soc.* **2012**, *134*, 7266-7269.
- (25) Turkevich, J. *Gold Bulletin* **1985**, *18*, 86-91.
- (26) Ziebacz, N.; Wieczorek, S. A.; Kalwarczyk, T.; Fialkowski, M.; Holyst, R. *Soft Matter* **2011**, *7*, 7181-7186.
- (27) Zaki, A.; Dave, N.; Liu, J. *J. Am. Chem. Soc.* **2012**, *134*, 35-38.
- (28) Zhang, X.; Huang, P.-J. J.; Servos, M. R.; Liu, J. *Langmuir* **2012**, *28*, 14330-14337.
- (29) Hurst, S. J.; Hill, H. D.; Mirkin, C. A. *J. Am. Chem. Soc.* **2008**, *130*, 12192-12200.

- (30) Jin, R.; Wu, G.; Li, Z.; Mirkin, C. A.; Schatz, G. C. *J. Am. Chem. Soc.* **2003**, *125*, 1643-1654.
- (31) Eryazici, I.; Prytkova, T. R.; Schatz, G. C.; Nguyen, S. T. *J. Am. Chem. Soc.* **2010**, *132*, 17068-17070.
- (32) Gibbs-Davis, J. M.; Schatz, G. C.; Nguyen, S. T. *J. Am. Chem. Soc.* **2007**, *129*, 15535-15540.
- (33) Storhoff, J. J.; Lazarides, A. A.; Mucic, R. C.; Mirkin, C. A.; Letsinger, R. L.; Schatz, G. C. *J. Am. Chem. Soc.* **2000**, *122*, 4640-4650.
- (34) Saeki, S.; Kuwahara, N.; Nakata, M.; Kaneko, M. *Polymer* **1976**, *17*, 685-689.
- (35) Busby, T. F.; Ingham, K. C. *Vox Sanguinis* **1980**, *39*, 93-100.
- (36) Kenkare, P. U.; Hall, C. K. *AIChE Journal* **1996**, *42*, 3508-3522.